Supplementary Materials and Methods

Ceramides Dissociate Steatosis and Insulin Resistance in the Human Liver in Non-Alcoholic Fatty Liver Disease

Panu K. Luukkonen[1, 2*], You Zhou[1*], Sanja Sädevirta[1, 2], Marja Leivonen[3], Johanna Arola[4], Matej Orešič[5], Tuulia Hyötyläinen[5], Hannele Yki-Järvinen[1, 2]

[1]Minerva Foundation Institute for Medical Research, Helsinki, Finland, [2]Department of Medicine, [3]Department of Surgery and [4]Department of Pathology, University of Helsinki and Helsinki University Hospital, Helsinki, Finland, [5]Steno Diabetes Center, Gentofte, Denmark

**These authors contributed equally to this work*

Table of Contents

Lipidomics analysis

Lipidomics using UHPLC-MS was performed at VTT Technical Research Centre of Finland (Espoo, Finland). Liver tissue (approximately 5 mg) was first homogenized when still frozen (Covaris, CryoPrep CP02, MA), and weighted. An aliquot (20 µL) of an internal standard mixture containing PC(17:0/0:0), PC(17:0/17:0), PE(17:0/17:0), phosphatidylglycerol(17:0/17:0)[rac], Ceramide(d18:1/17:0), PS(17:0/17:0), phosphatidic acid(17:0/17:0) (Avanti Polar Lipids, Alabaster, AL), monoacylglycerol(17:0/0:0/0:0)[rac], DAG(17:0/17:0/0:0)[rac] and TAG(17:0/17:0/17:0) were added. The lipids were extracted using a mixture of HPLC-grade chloroform and methanol (2:1; 400 µL). 50 µl of 0.9% NaCl was added and the lower phase (200 µL) was collected and 20 µL of an internal standard mixture containing labeled PC(16:1/0:0-D_3), PC(16:1/16:1-D_6) and TAG(16:0/16:0/16:0-$^{13}C3$) was added. The extracts were run on a Waters Q-TOF Premier mass spectrometer combined with an Acquity Ultra Performance LC™ as described earlier (1).

The column (at 50 °C) was an Acquity UPLC™ BEH C18 2.1 × 100 mm with 1.7 µm particles. The solvent system included A. ultrapure water (1% 1 M NH_4Ac, 0.1% HCOOH) and B. LC/MS grade acetonitrile/isopropanol (1:1, 1% 1M NH_4Ac, 0.1% HCOOH). The gradient started from 65% A / 35% B, reached 80% B in 2 min, 100% B in 7 min and remained there for 7 min. The flow rate was 0.400 ml/min and the injected amount was 2.0 µl (Acquity Sample Organizer, at 10 °C). Reserpine was used as the lock spray reference compound. The lipid profiling was carried out using electrospray ionization mode and the data were collected at a mass range of m/z 300-1200 with a scan duration of 0.2 sec.

The data processing included alignment of peaks, peak integration, normalization and identification. Lipids were identified using an internal spectral library. The data were normalized using one or more internal standards representative of each class of lipid present in the samples: the intensity of each identified lipid was normalized by dividing it with the intensity of its corresponding standard and multiplying it by the concentration of the standard. All monoacyl lipids except cholesterol esters, such as monoacylglycerols and monoacylglycerophospholipids, were normalized with PC(17:0/0:0), all diacyl lipids except ethanolamine phospholipids were normalized with PC(17:0/17:0), all ceramides with Cer(d18:1/17:0), all diacyl ethanolamine phospholipids with PE(17:0/17:0), and TAG and cholesterol esters with TAG(17:0/17:0/17:0). Other (unidentified) molecular species were normalized with PC(17:0/0:0) for retention times < 300 s, PC(17:0/17:0) for a retention time between 300 s and 410 s, and TAG(17:0/17:0/17:0) for longer retention times.

Quality control of the method showed that the day-to-day repeatability of control serum samples, and the relative standard deviation (RSD) for identified lipids was on average 14.1% in ESI+ mode and 9.5% in ESI- mode. The internal standards added to all samples (n=125) in the study had an average RSD of 10.8% in ESI+ mode and 8.0% in ESI- mode.

Analysis of hepatic free fatty acids

Fatty acid analysis was performed at VTT Technical Research Centre of Finland (Espoo, Finland). Liver tissue was first homogenized when still frozen (Covaris, CryoPrep CP02, MA) and weighted (ca. 10 mg). The homogenate was spiked with 10 µl of internal standard mixture (DL-Valine at 37 mg/l, heptadecanoic acid at 186.5

mg/l, succinic acid-d4 at 62.9 mg/l and DL-Glutanic acid-d5 at 103.5 mg/l) and the samples were extracted with 400 µl MeOH/H2O 1:1 (v/v). The supernatant was collected and evaporated to dryness under gentle flow of nitrogen. The fatty acids were then converted into their methoxime (MEOX) and trimethylsilyl (TMS) derivative(s) by two-step derivatization and analyzed as described earlier (2). First, 25 µL of MOX reagent was added to the residue, and the mixture was incubated for 60 min at 45 °C. Next, 25 µL of MSTFA was added, and the mixture was incubated for 60 min at 45 °C. Finally, a retention index standard mixture (n-alkanes) and an injection standard (4,4'-dibromooctafluorobiphenyl), both in hexane, were added to the mixture.

GC×GC–TOFMS experiment were carried out on an Agilent 6890 gas chromatograph equipped with a split/splitless injector (Agilent Technologies, Santa Clara, CA), cryogenic dual-stage modulator and time-of-flight mass spectrometer (Leco Corp., St. Joseph, MI, USA). In addition, multipurpose sampler with Maestro software (Gerstel, Mülheim an der Ruhr, Germany) was used for derivatization and sample introduction. A 10 m × 0.18 mm I.D. Rxi-5ms (Restek Corp., Bellefonte, PA, USA) column with film thickness 0.18 µm was used as the first column and a 1.5 m × 0.1 mm I.D. BPX-50 (SGE Analytical Science, Austin, TX, USA) column with film thickness of 0.1 µm as the second column. A phenyl methyl deactivated retention gap column (1.5 m × 0.53 mm I.D.) was installed in front of the first column. The injector was used in the splitless mode at 240 °C for injecting 1 µl of a sample. The splitless period was 90 s. High-purity helium (Aga, Espoo, Finland) was used as the carrier gas in a constant-pressure mode with initial pressure of 276 kPa. The first column oven temperature program was as follows: 50 °C (isothermal for 2 min) then 7 °C/min to 240 °C, and,

finally, 25 °/min to 300 °C (3 min). The second dimension column oven temperature was maintained 20 °C higher and the programming rate and hold times were similar than in the first dimension. The temperature of the transfer line was maintained at 260 °C and ion source at 200 °C. Modulation time was 4 s. Electron impact ionization was applied at 70 eV, and the mass range from 45 to 700 amu with 100 spectra/s were measured.

Automatic peak detection and mass spectrum deconvolution were performed using a peak width set to 0.2 s. Peaks with signal-to-noise (S/N) values lower than 100 were rejected. The S/N values were based on the masses chosen by the software for quantification. ChromaTOF version 4.32 was used for the raw data processing. The peak areas from total ion chromatography (TIC) were used for most of the compounds; for compounds that were quantified with the ChromaTOF software, peak areas of selected characteristic m/z were used.

Next, the data files obtained by the ChromaTOF software were exported to text files and in-house developed software Guineu16 was used for aligning and normalization of compounds in different data sets for further analyses. The original GC×GC–TOFMS data includes retention times, retention indices (I), spectral information for possible identification, spectral similarity value (S=0-999), and peak response data. The linear retention indices were calculated based on the total (=sum of the first and the second dimension) retention times of the compounds and the retention times of the retention index standards (n-alkanes). The second dimension retention time is so short (1-3.5 s) that its contribution to the retention index is not significant. The alignment of the data was performed based on retention indices, second dimension retention times

and spectra. After alignment of the GC×GC–TOFMS data, two filtration criteria was utilised for positive identification: spectral similarity > 850 and maximum allowed difference in retention index between experimental and literature values < 25. The literature values were obtained from NIST 2008 Mass Spectral Library or they were determined experimentally with GC×GC-TOFMS instrument in our laboratory with authentic standards (in-house determined library). In addition, Golm metabolome database was used for further identification of the metabolites.

Quantitation was based on external calibration of each specific fatty acid, normalised by the internal standard. Quality control of the method showed that the day-to-day repeatability of control serum samples, and the relative standard deviation (RSD) for fatty acids was on average 10.3%. The internal standards added to all samples (n=125) in the study had an average RSD of 12.3%.

Cluster analysis of liver lipidome

A total of 1458 lipids were measured and 324 identified. The lipidomic data were decomposed into 11 lipid clusters (LCs), which largely adhered to different functional or structural groups of lipids (Supplementary Table 1). After log2 transformation, lipidomics data of each lipid species were scaled to zero mean and unit variance. The average profile of each cluster was represented by the mean value of all lipids contained. The comparisons of clusters between subgroups ('High HOMA-IR' *vs.* 'Low HOMA-IR'; 'PNPLA3$^{148MM/MI}$' *vs.* 'PNPLA3^{148II}') were visualized by bar plots (Supplementary Fig. 2).

In the 'High HOMA-IR' compared to the 'Low HOMA-IR', LCs containing ceramides and dihydroceramides (LC1), DAGs, saturated and monosaturated TAGs (LC5), and polyunsaturated TAGs (LC8, LC10 and LC11) were increased (Supplementary Table 1 and Supplementary Fig. 2, top panel). In the PNPLA3$^{148MM/MI}$ compared with the PNPLA3^{148II} group, LC1 and LC5 were not different (Supplementary Fig. 2, bottom panel). Clusters containing mostly polyunsaturated TAGs (LC8, LC9, LC10 and LC11) differed significantly (Supplementary Table 1 and Supplementary Fig. 2, bottom panel). These lipid species (TAGs, DAGs, ceramides and dihydroceramides) were therefore the focus for further analysis.

Assessment of abundances of lipid species

After log2 transformation, the mean values of concentrations of all lipids were compared between subgroups based on HOMA-IR and PNPLA3 genotype. The multiple hypotheses testing was done by Benjamini-Hochberg's method (30). The comparisons of concentrations of TAGs and DAGs were illustrated by heatmaps, which plot chain length against the number of double bonds. The comparisons of concentrations of ceramides and their precursors were illustrated by heatmaps, which plot fatty acyl chain against sphingoid base. The color intensity of each cell in the heatmap represents the log2 transformed ratio of mean values of individual lipid molecules of the cases divided by the controls.

HOMA-IR cut-off for NASH

To determine the HOMA-IR cut-off differentiating subjects with and without NASH, the subjects were randomly divided into discovery (n=83) and validation cohorts (n=42) to build and validate the model, respectively. All study subjects were used as a second validation cohort (n=125). The optimal cut-off was calculated using the Youden index. The HOMA-IR value with best sensitivity and specificity was equal to 3.379. The area under the receiver operating characteristic curve was 0.6788 (0.5635 – 0.7941), sensitivity was 0.72 and specificity was 0.62. The positive predictive value of the cut-off was 0.321 and the negative predictive value was 0.899.

Paired analyses of HOMA-IR and PNPLA3 with 4 groups

In addition to dividing the subjects into 2 groups separately based on median HOMA-IR and based on the PNPLA3 I148M genotype, we also divided the subjects simultaneously into 4 groups based on these 2 risk factors of NAFLD ('High HOMA-IR and PNPLA3$^{148MM/MI}$', 'High HOMA-IR and PNPLA3^{148II}', 'Low HOMA-IR and PNPLA3$^{148MM/MI}$' and 'Low HOMA-IR and PNPLA3^{148II}' groups (Supplementary Fig. 1). Comparison of 'High HOMA-IR and PNPLA3$^{148MM/MI}$' vs. 'Low HOMA-IR, PNPLA3$^{148MM/MI}$' was used to study the impact of insulin resistance alone on the liver lipidome. Comparison of 'High HOMA-IR and PNPLA3$^{148MM/MI}$' vs. 'High HOMA-IR, PNPLA3^{148II}' group was used to study the effect of the PNPLA3 I148M gene variant alone on the liver lipidome.

Characteristics of the study groups

Characteristics of the four subgroups based on simultaneous division by median HOMA-IR and the PNPLA3 I148M genotype are shown in Supplementary Table 2. All groups had similar age, gender and BMI (Supplementary Table 2, Supplementary Fig. 6).

Impact of insulin resistance on the liver lipidome

The 'High HOMA-IR and PNPLA3$^{148MM/MI}$' group had higher waist circumference, HOMA-IR and fasting serum insulin, plasma glucose, triglycerides and ALT concentrations as compared to the 'Low HOMA-IR and PNPLA3$^{148MM/MI}$' group (Supplementary Table 2, Supplementary Fig. 6). The former group also had higher liver fat and NASH % (Supplementary Table 2, Supplementary Fig. 6) as compared to

the latter group. The distribution of PNPLA3 genotype was similar in both subgroups (Suppl. Table 2).

Impact of the PNPLA3 I148M gene variant on the liver lipidome

The 'High HOMA-IR and PNPLA3$^{148MM/MI}$' group had higher NASH % and AST concentration and lower platelet count as compared to the 'High HOMA-IR and PNPLA3^{148II}' group. Liver fat displayed increasing trend in the former as compared to the latter group, but the difference did not reach significance (Supplementary Table 2, Supplementary Fig. 6). Waist circumference, HOMA-IR, fasting serum insulin, plasma glucose and triglycerides were similar in the subgroups (Supplementary Fig. 6).

Liver TAGs

The livers in 'High HOMA-IR and PNPLA3$^{148MM/MI}$' vs. 'Low HOMA-IR and PNPLA3$^{148MM/MI}$' group were enriched in TAGs containing 48-60 carbons and 0-5 double bonds (Supplementary Fig. 7, panel on the left). In 'High HOMA-IR and PNPLA3$^{148MM/MI}$' vs. 'High HOMA-IR and PNPLA3^{148II}' group, the livers were enriched in TAGs containing 50-60 carbons and 3-11 double bonds (Supplementary Fig. 7, panel on the right).

Liver ceramides

Concentrations of 14 out of 17 ceramide species were significantly increased in the livers of the 'High HOMA-IR and PNPLA3$^{148MM/MI}$' vs. 'Low HOMA-IR and PNPLA3$^{148MM/MI}$' group (Supplementary Fig. 8, panel on the left). Hepatic ceramide

concentrations were similar in the ‘High HOMA-IR and PNPLA3$^{148MM/MI}$, vs. ‘High HOMA-IR and PNPLA3^{148II}, groups (Supplementary Fig. 8, panel on the left).

Supplementary Figures

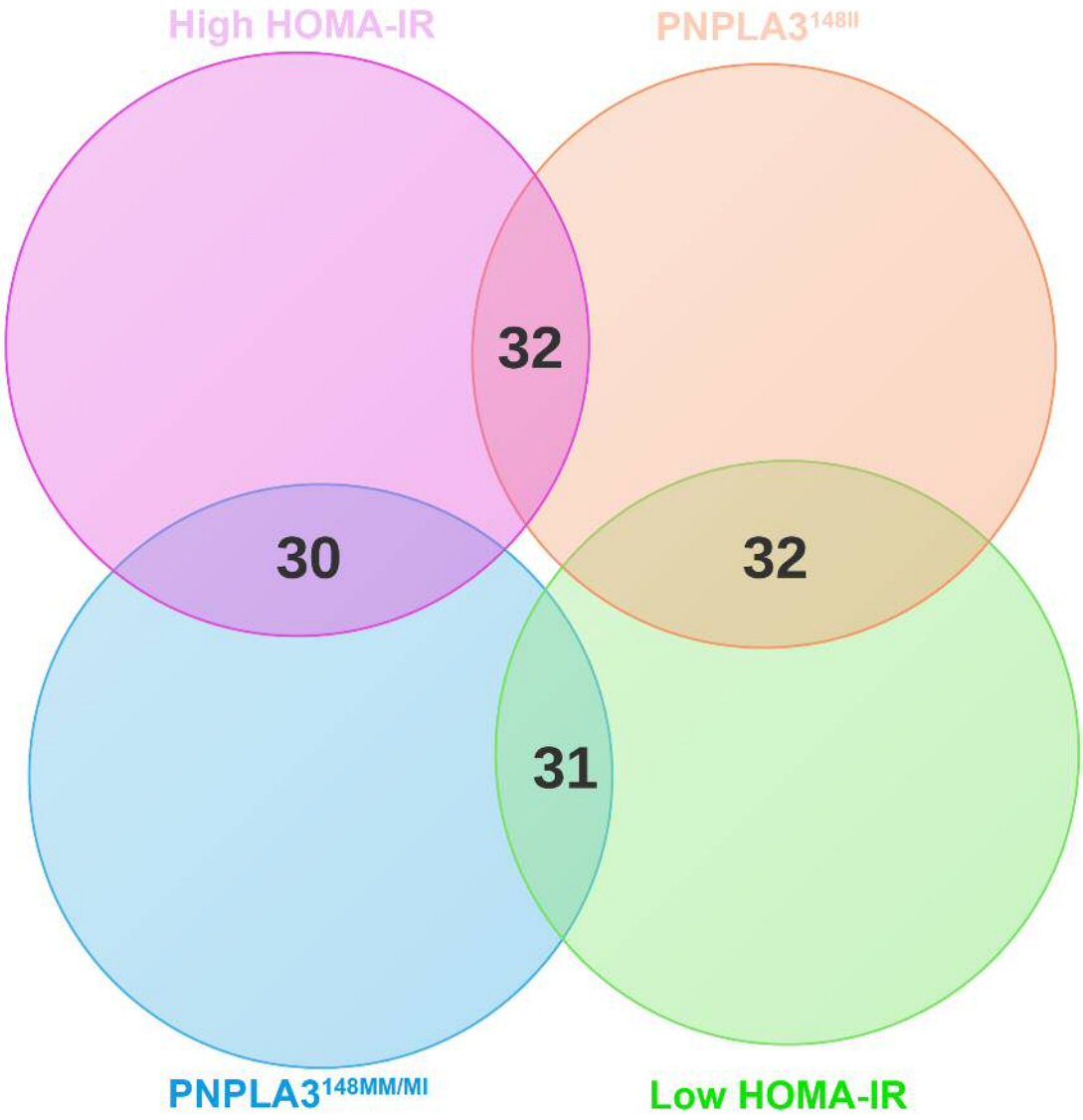

Supplementary Fig. 1. A four-circle Venn diagram illustrating the allocation of the subjects to groups. The sum of numbers inside each circle denotes the total number of subjects in a group. The numbers in the overlapping areas of a circle denote the division of the subjects into subgroups (i.e. 'High HOMA-IR' group has a total of 62 subjects, of whom 32 are also included into 'PNPLA3^{148II}' group and 30 into 'PNPLA3$^{148MM/MI}$' group).

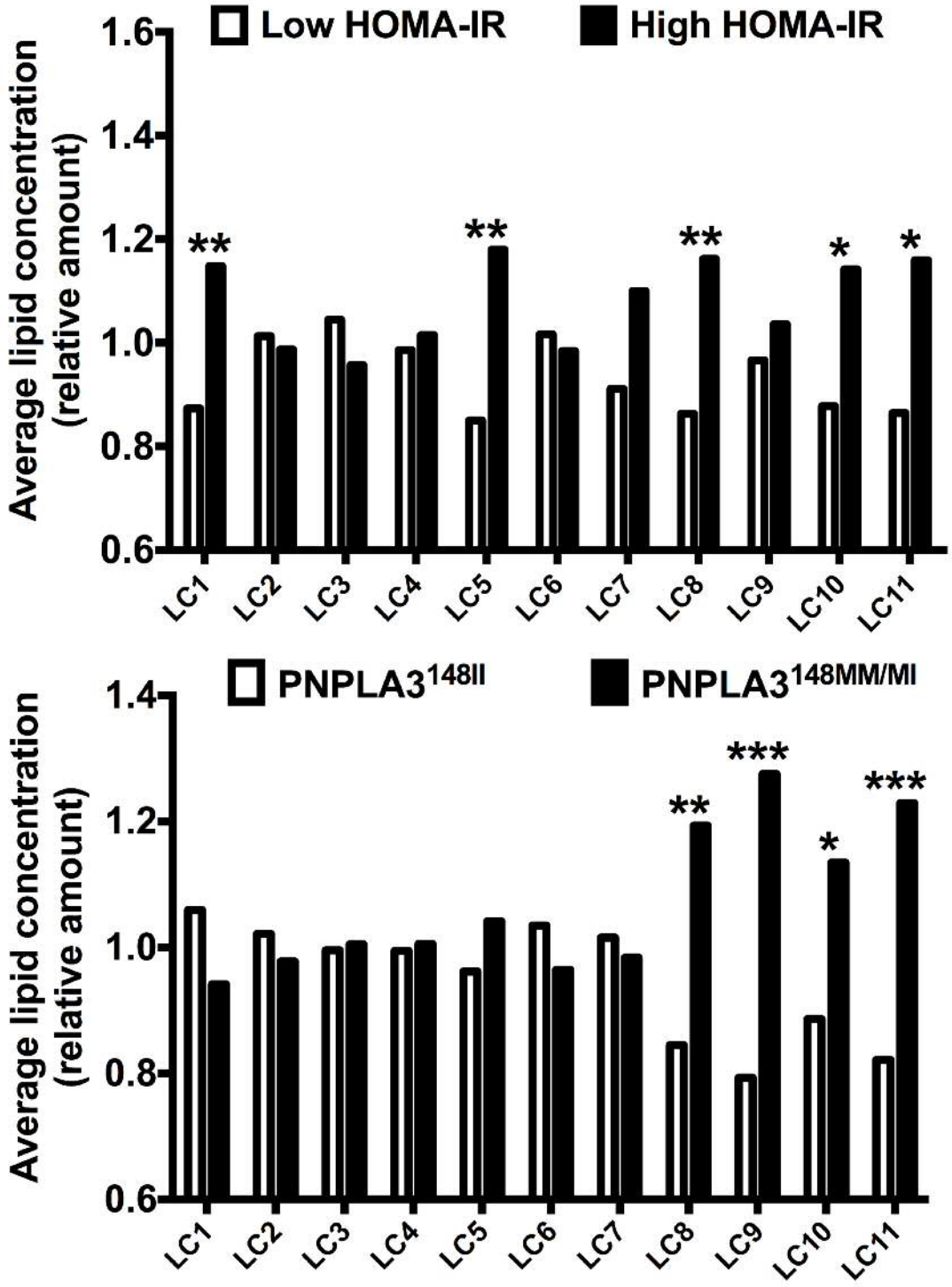

Supplementary Fig. 2. Mean scaled lipid concentrations within each cluster between 'High HOMA-IR' and 'Low HOMA-IR' groups (upper panel) and between 'PNPLA3$^{148MM/MI}$' and 'PNPLA3^{148II}' groups (lower panel). Statistical comparison performed by two-sided t test. *p<0.05, **p<0.01, ***p<0.001.

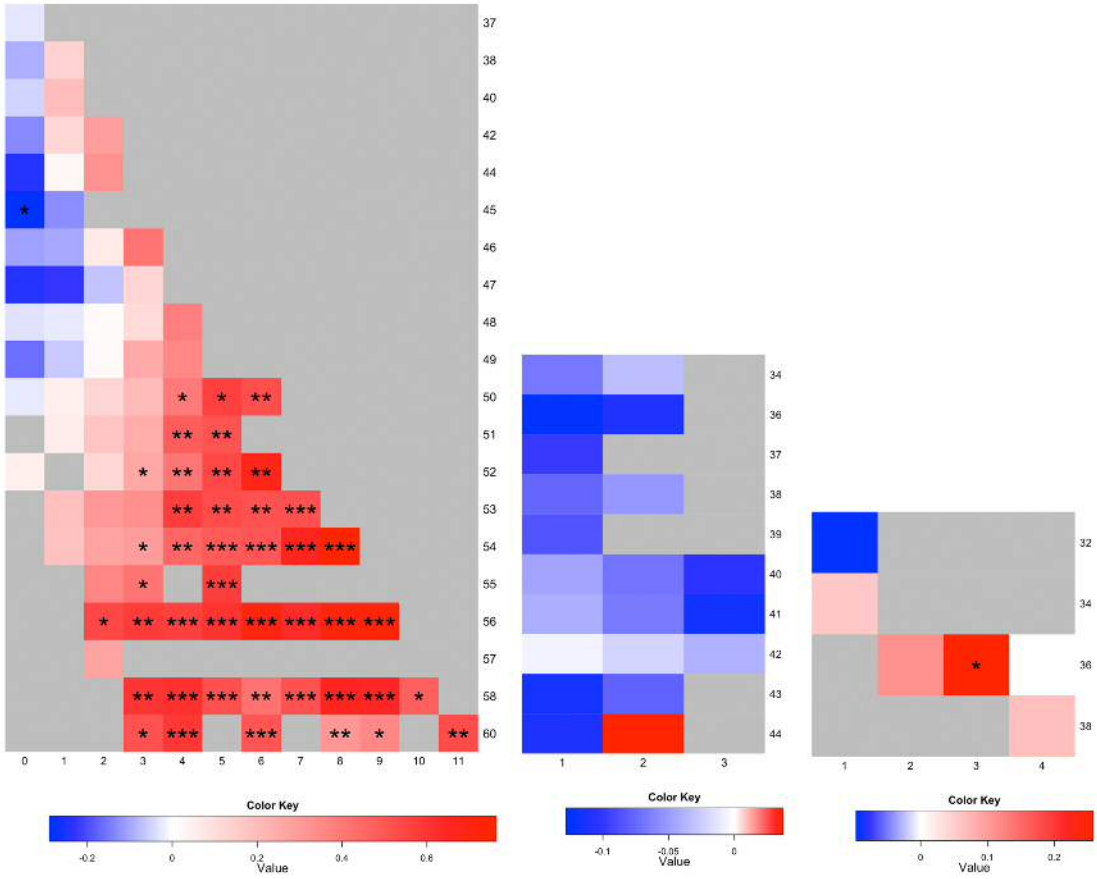

Supplementary Fig. 3. Absolute concentrations of hepatic TAGs, ceramides and DAGs in 'PNPLA3$^{148MM/MI}$' vs. 'PNPLA3^{148II}' within the 'Low HOMA-IR' subgroup only (TAGs, panel on the left; ceramides, panel in the middle; DAGs, panel on the right). The color code represents the log of the ratio between means of the groups for an individual lipid species. The y-axes denote the number of carbons and the x-axes the number of double bonds. The brighter the red color, the greater increase of absolute concentration of the individual lipid in the 'PNPLA3$^{148MM/MI}$' compared to the 'PNPLA3^{148II}' group. *p<0.05, **p<0.01, ***p<0.001.

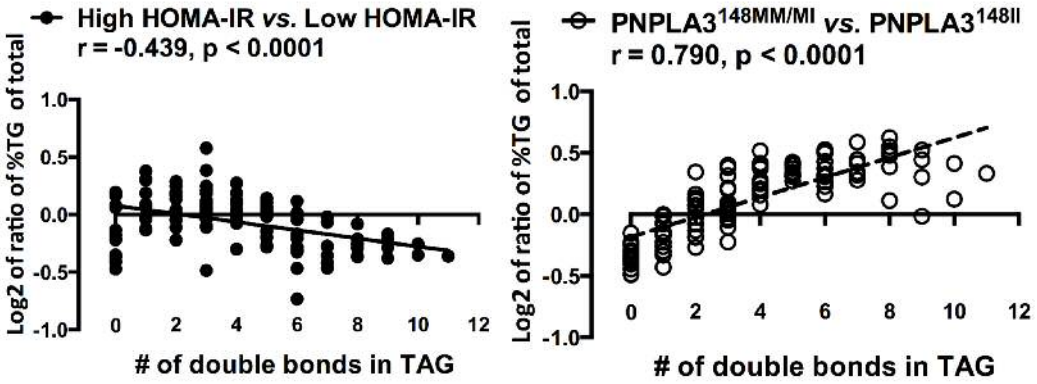

Supplementary Fig. 4. Relationships between fold changes of relative concentrations of individual TAGs and the double bonds contained.

To further compare liver TAG composition independent of total TAGs, relative TAGs concentrations were calculated by dividing the concentration of each individual TAG by total TAG amount as measured by UHPLC-MS. The x-axis shows the number of double bonds in TAGs, and the y-axis the log2 of the ratio of relative abundances of TAGs between 'High HOMA-IR' and 'Low HOMA-IR' groups (left panel) and between 'PNPLA3$^{148MM/MI}$' and 'PNPLA3^{148II}' groups (right panel). Each dot represents an individual TAG. The fold-changes of relative TAG concentrations between 'High' and 'Low HOMA-IR' groups were inversely correlated with their number of double bonds (r = -0.439, $p < 0.0001$, panel on the left). In contrast, fold-changes of relative levels of individual TAGs between the PNPLA3$^{148MM/MI}$ and PNPLA3^{148II} groups were positively correlated with the number of double bonds (r = 0.790, $p < 0.0001$, panel on the right).

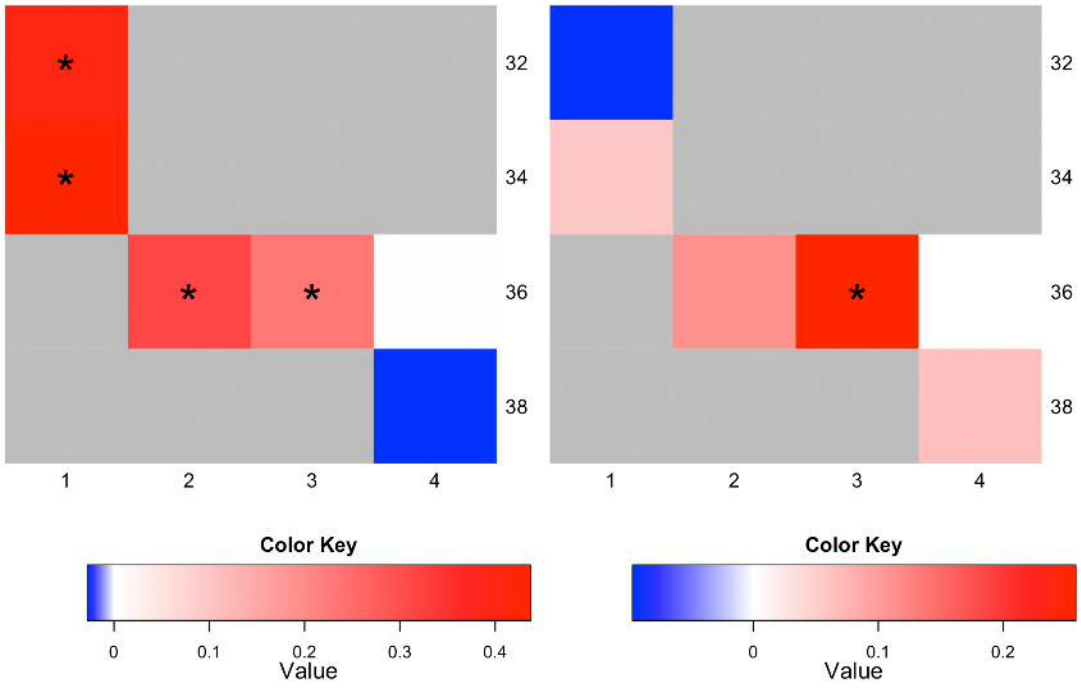

Supplementary Fig. 5. Absolute concentrations of hepatic DAGs between groups ('High HOMA-IR' *vs.* 'Low HOMA-IR', panel on the left; 'PNPLA3$^{148MM/MI}$' *vs.* 'PNPLA3^{148II}' groups panel on the right). The color code indicates the log of the ratio between means of the groups for an individual DAG. The y-axes denote the number of carbons and the x-axes the number of double bonds. The red color indicates the increase of absolute concentration of the DAG and the blue represents the decrease. *p<0.05.

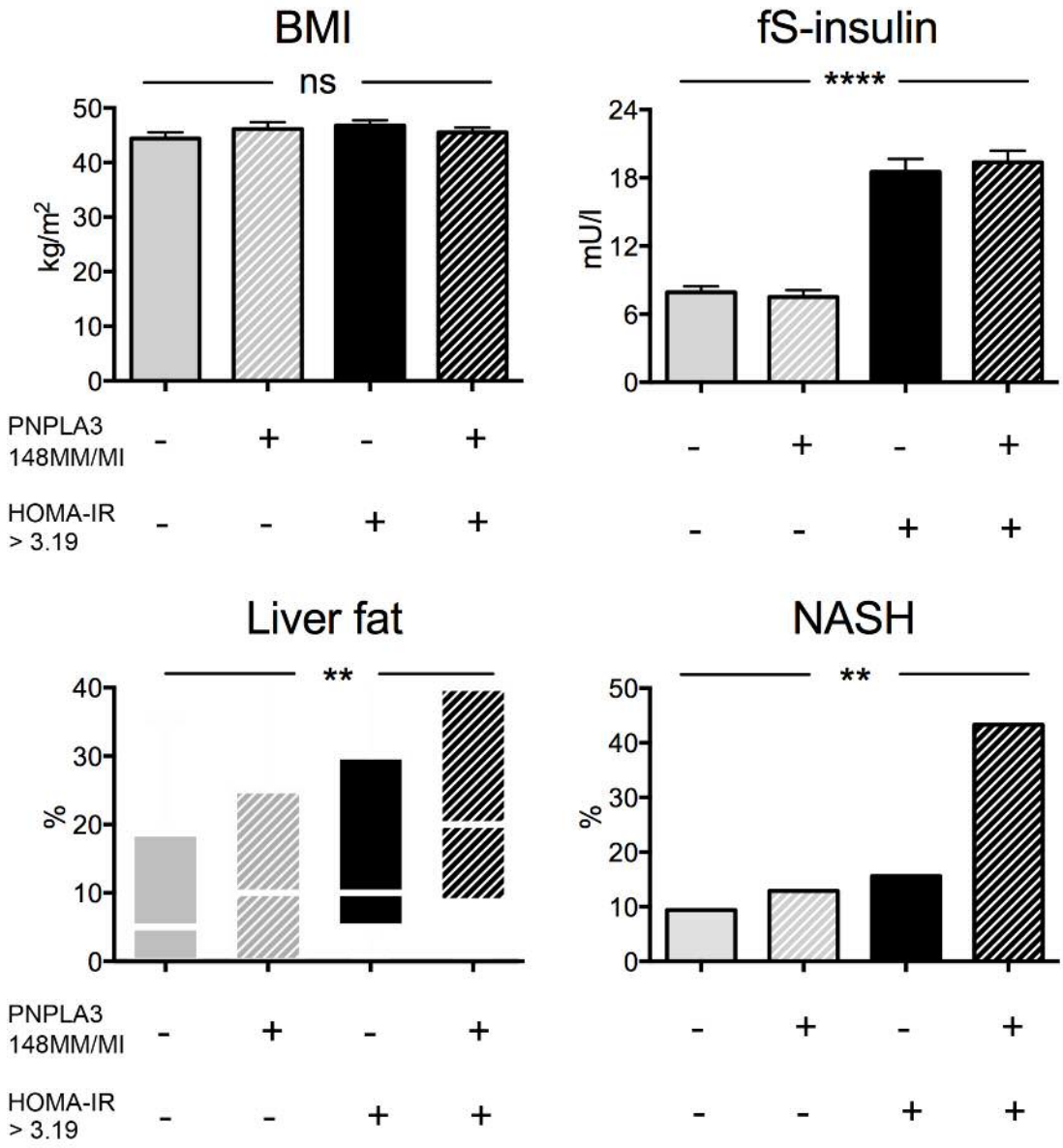

Supplementary Fig. 6. BMI (upper left panels), fasting serum insulin (upper right panels), liver fat (lower left panels) and prevalence of NASH (lower right panels) in four non-overlapping subgroups based on the PNPLA3 I148M genotype and HOMA-IR. Data are shown in mean ± SEM for BMI and fS-insulin, and in medians and interquartile ranges for liver fat. 'ns' $p>0.05$, ** $p<0.01$, **** $p<0.0001$.

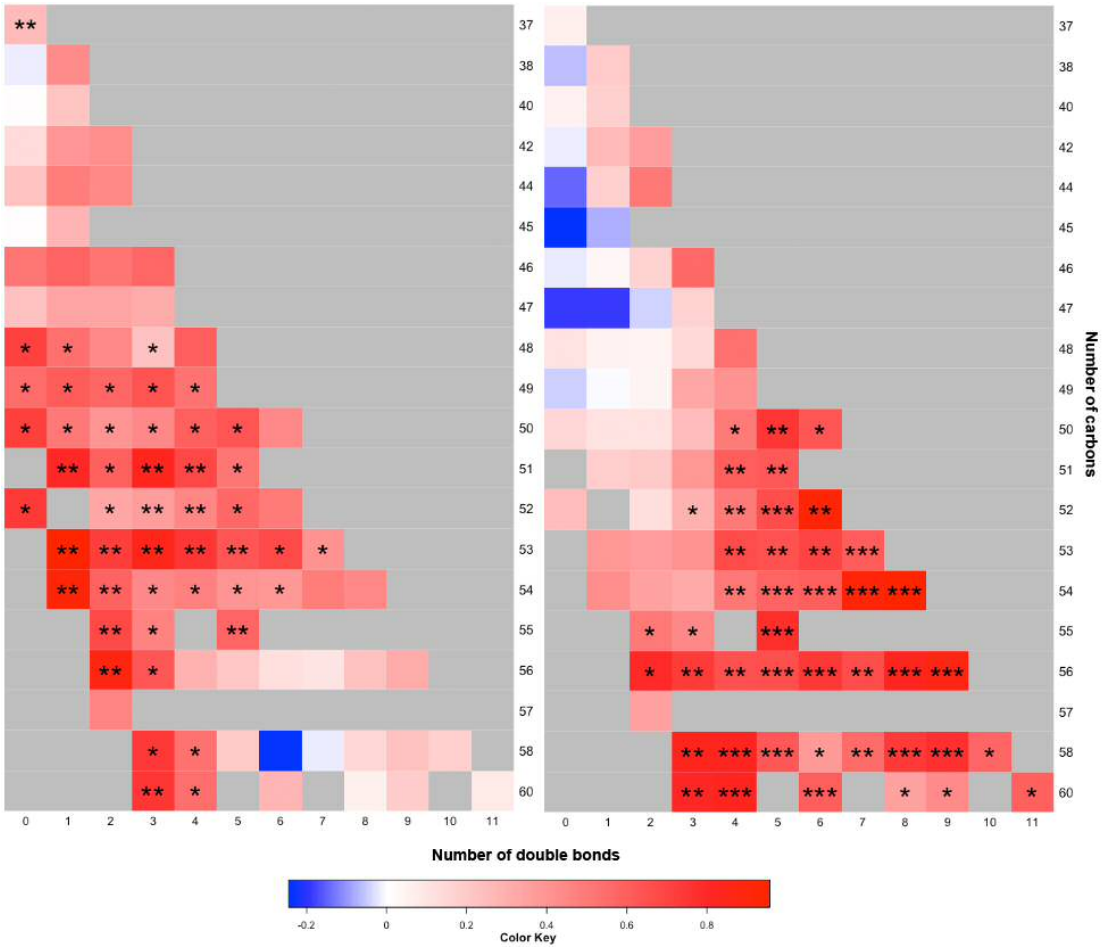

Supplementary Fig. 7. Absolute concentrations of hepatic TAGs between 'High HOMA-IR and PNPLA3$^{148MM/MI}$, vs. 'Low HOMA-IR and PNPLA3$^{148MM/MI}$, (panel on the left) and between 'High HOMA-IR and PNPLA3$^{148MM/MI}$, vs. 'High HOMA-IR and PNPLA3^{148II}, (panel on the right). The color code indicates the log of the ratio between means of the groups for an individual TAG. The y-axes denote the number of carbons and the x-axes the number of double bonds. The red color indicates the increase of absolute concentration of the TAG and the blue represents the decrease. *p<0.05, **p<0.01, ***p<0.001.

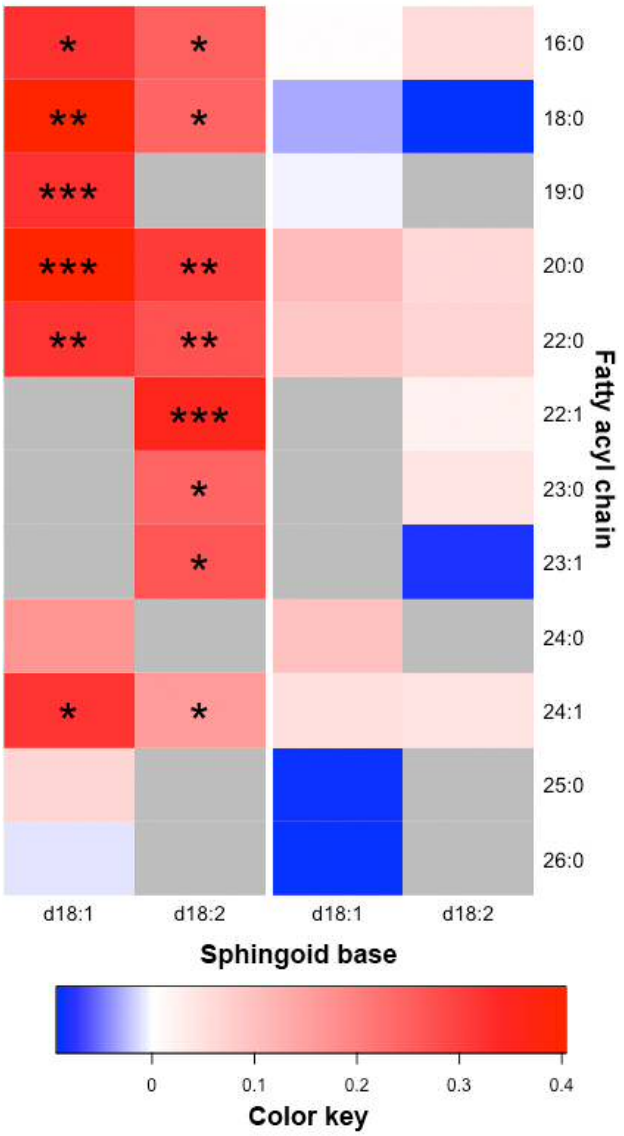

Supplementary Fig. 8. Absolute concentrations of hepatic ceramides between 'High HOMA-IR and PNPLA3$^{148MM/MI}$' vs. 'Low HOMA-IR and PNPLA3$^{148MM/MI}$' (panel on the left) and between 'High HOMA-IR and PNPLA3$^{148MM/MI}$' vs. 'High HOMA-IR and PNPLA3^{148II}' (panel on the right). The color code indicates the log of the ratio between means of the groups for an individual ceramide. The y-axes denote the fatty acyl chain and the x-axes sphingoid base in the given ceramide molecule. The red color indicates the increase of absolute concentration of the ceramide and the blue represents the decrease. *p<0.05, **p<0.01, ***p<0.001.

Supplementary Table 1. Composition of hepatic lipid clusters

Cluster name	Size	Representative members
LC1	31	CER(d17:1/22:0); CER(d17:1/24:1) + CER(d18:2/23:0)+ CER(d18:1/23:1); CER(d18:0/16:0); CER(d18:0/18:0); CER(d18:0/23:0); CER(d18:0/24:0); CER(d18:0/24:1)
LC2	47	PC(16:0/20:4); PC(16:1/20:4); PC(18:0/20:4); PE(16:0/20:4)+ PE(18:2/18:2); PE(18:0/20:4); PE(36:2); HexCER(d18:1/24:0); SM(d18:1/14:0); SM(d18:1/15:0); SM(d18:1/16:0); SM(d18:1/16:1); SM(d18:1/17:0); SM(d18:1/18:0); SM(d18:1/20:0); SM(d18:1/21:0)
LC3	32	PC(16:0/16:1)+PC(14:0/18:1); PC(16:0/20:5); PC(18:1/20:4); PE(36:5); PE(38:6); PE(38:6); PE(40:5)+PC(37:5)
LC4	49	PC(36:3e); PC(38:5e); PC(40:5e); PC(p16:0/16:0); PC(p18:0/20:4); PE(18:0/22:4); PE(34:0); PE(38:6e); PE(p16:0/18:1); PE(p16:0/18:1)
LC5	25	DAG(32:1); DAG(34:1); DAG(36:2); TAG(16:0/16:0/16:0)+TAG(14:0/16:0/18:0); TAG(48:1); TAG(49:1);TAG(50:0); TAG(50:1); TAG(51:1); TAG(52:0)
LC6	51	PC(16:0/16:1)+PC(14:0/18:1); PC(16:0/18:1); PC(18:1/18:0); PE(16:0/16:1); PE(18:0/18:1); PE(18:0/20:3)
LC7	21	TAG(38:1); TAG(40:1); TAG(42:0); TAG(42:1); TAG(42:2)

LC8	18	TAG(17:1/18:1/18:2); TAG(18:1/18:1/18:1); TAG(18:1/18:1/22:1)+ TAG(20:1/20:1/18:1); TAG(18:1/18:2/18:1)
LC9	28	TAG(22:6/18:1/18:1); TAG(52:6); TAG(54:6); TAG(54:7); TAG(54:8)
LC10	12	TAG(46:3); TAG(47:3); TAG(48:3); TAG(48:4); TAG(49:3)
LC11	10	TAG(51:4); TAG(51:5); TAG(52:4); TAG(52:5); TAG(53:5)

Supplementary table 2. Clinical characteristics of the study subjects according to the PNPLA3 genotype at rs738409 and HOMA-IR.

Total	HOMA-IR > 3.19, PNPLA3$^{148MM/MI}$ (n=30)	HOMA-IR > 3.19, PNPLA3^{148II} (n=32)	HOMA-IR <3.19, PNPLA3$^{148MM/MI}$ (n=31)	HOMA-IR <3.19, PNPLA3^{148II} (n=32)
Age (years)	47.9 ± 1.5	44.7 ± 1.5	50.6 ± 1.2	47.8 ± 1.7
Gender (n, % women)	15 (50.0)	23 (71.9)	23 (74.2)	22 (68.8)
Waist circumference (cm)	137.5 ± 2.3	133.6 ± 2.3	128.4 ± 2.5**	126.8 ± 2.7**
fP-Glucose (mmol/l)	6.1 (5.7 - 6.8)	6.1 (5.4 - 6.9)	5.5 (4.4 – 5.9)***	5.6 (4.8 - 6.0)**
HbA_{1C} (%)	6.0 (5.7 - 6.7)	6.0 (5.6 - 6.4)	5.7 (5.5 - 6.2)	5.7 (5.4 - 6.1)
HOMA-IR	5.1 (4.1 – 5.8)	4.5 (3.6 – 5.7)	1.7 (1.4 – 2.4)***	1.9 (1.2 – 2.7)***
Matsuda ISI	34.3 (27.4 – 44.0)	36.6 (27.1 – 47.5)	95.6 (60.0 – 168.3)***	85.9 (66.8 – 139.6)***
fP-Triglycerides (mmol/l)	1.29 (1.06 - 1.56)	1.53 (1.24 – 2.12)	1.14 (0.94 - 1.78)	1.09 (0.88 - 1.46)
fP-HDL cholesterol (mmol/l)	1.04 (0.88 - 1.23)	1.00 (0.93 - 1.16)	1.13 (1.03 - 1.44)	1.19 (1.00 - 1.43)*
fP-LDL cholesterol (mmol/l)	2.4 ± 0.2	2.6 ± 0.1	2.5 ± 0.2	2.4 ± 0.1
Liver fat (%)	20 (9 - 40)	10 (5 - 30)	10 (5 - 25)**	5 (0 - 19)***
P-AST (IU/l)	34 (27 - 49)	28 (24 - 33)**	31 (25 - 38)	26 (24 - 35)*
P-ALT (IU/l)	41 (31 - 52)	36 (29 - 49)	35 (20 - 41)**	26 (22 - 32)***
P-ALP (IU/l)	62 ± 3	67 ± 2	66 ± 4	65 ± 3
P-GGT (U/l)	41 (24 - 53)	33 (21 - 50)	27 (19 - 45)	26 (19 - 33)*
P-Albumin (g/l)	37.9 (36.1 - 39.0)	38.2 (36.1 – 40.5)	37.8 (36.0 – 39.5)	37.6 (36.8 - 39.4)
B-Platelets ($x10^9$/l)	228 ± 10	274 ± 11**	252 ± 11	241 ± 13
PNPLA3 (CC/CG/GG) (n)	0/27/3	32/0/0***	0/27/4	32/0/0***
Use of statins (n, %)	11 (36.7)	11 (34.4)	7 (22.6)	11 (34.4)
NASH (%)	43.3	15.6*	12.9**	9.4**

Data are in n (%), means ± SEM or median (25th-75th percentile), as appropriate. For *t* test, Mann-Whitney test and Pearson chi-square test against the 'HOMA-IR > 3.19, PNPLA3$^{148MM/MI}$, group. * $P \leq 0.05$, ** $P \leq 0.01$, *** $P \leq 0.001$.

References

1. Nygren H, Seppänen-Laakso T, Castillo S, Hyötyläinen T, Oresic M. Liquid Chromatography-Mass Spectrometry (LC-MS)-Based Lipidomics for Studies of Body Fluids and Tissues. In: Metz TO, ed. Metabolic Profiling. Totowa, NJ: Humana Press; 2010. p. 247–257.

2. Castillo S, Mattila I, Miettinen J, Oresic M, Hyötyläinen T. Data Analysis Tool for Comprehensive Two-Dimensional Gas Chromatography/Time-of-Flight Mass Spectrometry. Anal. Chem. 2011;83:3058–3067.